



## **EVALUATION OF FLEXURAL BEHAVIOUR OF LOW DENSITY FIBRE REINFORCED CONCRETE USING DIGITAL IMAGE CORRELATION**

Ibeawuchi, John<sup>1,2</sup>, Moffatt, Edward<sup>1</sup> and Lloyd, Alan<sup>1</sup>

<sup>1</sup> University of New Brunswick, Canada

<sup>2</sup> John.ibeawuchi@unb.ca

**Abstract:** Fibre reinforced concrete over the years has gained popularity in structural applications through studies on its behaviour. Despite these studies there is the need to fully understand the flexural behaviour of fibre reinforced concrete (FRC). This paper presents the results of an experimental program to investigate the mechanical properties and post-cracking behaviour of FRC beams under four-point loading using digital image correlation (DIC) to monitor strain, displacement, and cracking. Expanded polystyrene low-density fibre reinforced concrete beams with steel and polypropylene fibre types at replacement levels of 0% and 0.5% by volume for each fibre type were cast and tested in flexure in accordance to ASTM C1609/C1609M-12. This experimental work detects the initiation and propagation of cracks on the specimens. It shows the failure mechanism, neutral axis shift and compression strain field of each beam. Results from the experiments showed that steel fibre produced a slight increase in compressive strength. However, flexural strength and post-peak ductility were significantly higher with the addition of either steel or plastic fibres. Steel fibre mixtures showed tension hardening behaviour while plastic fibre mixtures exhibited tension softening behaviour and a significant drop in peak load after first crack, which is a result of rapid crack propagation due to the low stiffness of the plastic fibres. DIC was used to measure displacement and strain fields and the values validate traditional LVDT measurements.

### **1 INTRODUCTION**

Concrete is the most widely used building material in the world and is attributed to its availability and economy. The use of conventional plain concrete can sometimes be limited because of its brittle nature and low tensile properties. To improve the tensile properties, it has become common practice to use reinforcement to carry the tensile stresses that may develop in concrete. Concrete reinforcement affects crack development and propagation as it bridges the cracks and improves the behaviour of the concrete in flexure. Recent developments and research have given an alternative to the use of reinforcement bars in the form of fibre reinforcement, which involves the addition of discontinuous discrete reinforcing fibres of different types and geometry to the concrete matrix. In some cases, fibre reinforcement can be used to replace traditional reinforcement such as welded fabric, however, it can also be used in combination with steel reinforcement. Various forms and types of fibres are available, however, steel and plastic are the most common for a wide range of structural applications including but not limited to slabs on grade, mining, tunnelling and excavation support applications rock slope stabilization (ACI 544-2010).

Many researchers have studied the effects of test method, fibre geometry, aspect ratio, fibre type and volume fraction of the use of fibres in concrete and on the post-cracking strength of fibre reinforced concrete

(FRC). Carbon fibre has been found to give high compressive and splitting tensile strengths while steel fibre gives higher flexural strength and toughness (Wu et al., 2003). In hybrid construction containing both steel and plastic fibres, the concrete has been shown to improve in both strength and flexural toughness (Wu et al., 2003). Rizzutti and Bencardino (2014) analyzed the effects of fibre volume fraction on the mechanical properties of steel FRC. They observed that the addition of fibres does not significantly affect the compressive strength of concrete. Song and Hwang (2004) observed that the compressive strength of fibre reinforced concrete reached a maximum strength at a replacement of 1.5% by volume. They also observed that the flexural strength, splitting tensile strength and toughness index of fibre reinforced concrete improved with increasing fibre volume fraction. Others have attempted to model the pull-out behaviour of fibres in order to predict the flexural response of FRC. The property/quality of the concrete matrix, the fibre type, content and geometry determine the mechanical properties of FRC (Robins et al., 2002). These mechanical properties can be characterized from the analysis of stress-strain curves and load-deflection plots of the FRC. The primary reason for adding fibres in concrete is to improve the ductility and post peak behaviour.

The use of strain gauges, extensometers, linear variable differential transducer (LVDT) sensors and cross head movement have been well used in experimental research for measuring the displacements and strains of concrete. These techniques are not very accurate in the estimation of strain fields or early crack detection and local failure processes in structural members. An alternative technique is the use of digital image correlation (DIC) analysis.

DIC is one of the full field non-contact optical techniques used in measuring displacements and strains in experimental mechanics. Other techniques include photo-elasticity, geometric moiré, moiré interferometry, holographic interferometry, speckle interferometry (ESPI), and the grid method (Grédiac, 2004). These methods are however expensive, difficult to use and often cannot be used typically in outdoor conditions compared to DIC. DIC can be used in structural monitoring and inspections by capturing images and making comparisons/analysis to identify differences in the behaviour of a member under consideration. DIC is also a better alternative to methods like dye penetration in measuring crack opening (McCormick and Lord, 2010).

This paper presents an investigation into the behaviour of steel and polypropylene plastic FRC in flexure at a replacement level of 0.5% by volume. Behaviours were compared with a non-fibre low-density concrete mixture. This experimental work also validates the use of DIC in the measurement of displacement and strains as opposed to traditional methods of measurements. Low-density concrete containing expanded polystyrene (EPS) beads was used in the study due to its growth in popularity in the construction industry.

## 2 MATERIALS

All concrete mixtures were prepared with a general use (GU) ASTM C150 Type I Portland cement with a density of 3150 kg/m<sup>3</sup>. Concrete specimens were cast using a water/cement ratio (W/CM) of 0.35 in addition to a normal density gravel as the coarse aggregate with a nominal maximum size of 9.5 mm and a standard lab grade sand. In order to maintain a low W/C and reach a suitable strength, a moderate dosage of a high-range naphthalene-based superplasticizer was used to achieve a workable slump. Two types of fibres were studied including hooked end steel fibres glued together in bundles by a water soluble glue and polypropylene plastic fibres (see Table 1). The density of all mixtures, except the control, were reduced through the use of expanded polystyrene (EPS) beads with a nominal diameter of 6-10 mm.

Table 1: Properties of Fibres

|                        | Steel | Plastic |
|------------------------|-------|---------|
| Length $l_f$ (mm)      | 30    | 30      |
| Diameter $d_f$ (mm)    | 0.5   | 1.0     |
| $l_f/d_f$              | 60    | 30      |
| Tensile Strength (MPa) | 1500  | 800     |

### 3 MIX PROPORTIONS

Concrete mixtures were designed in accordance with ACI-211.2 and were modified by incorporating EPS beads. The expanded polystyrene beads were batched by volume as it was not accurate to batch by weight as a result of its low density. Two fibre volume contents of 0% (control) and 0.5% by volume were used. Table 2 presents the mix proportions of the various concrete mixes.

Table 2: Concrete Mix Proportions

| Mix     | Mix Designation | W/C  | Coarse Aggregate (kg/m <sup>3</sup> ) | Fine Aggregate (kg/m <sup>3</sup> ) | EPS Beads (m <sup>3</sup> ) | Cement (kg/m <sup>3</sup> ) | HRWRA (mL/100kg) | Fibre Volume (%) |
|---------|-----------------|------|---------------------------------------|-------------------------------------|-----------------------------|-----------------------------|------------------|------------------|
| Control | NFRNWC*         | 0.35 | 875                                   | 693                                 | -                           | 550                         | 975              | -                |
| Control | NFRLDC**        | 0.35 | 451                                   | 350                                 | 0.3                         | 550                         | -                | -                |
| Steel   | SFRLDC***       | 0.35 | 451                                   | 350                                 | 0.3                         | 550                         | 198              | 0.5              |
| Plastic | PFRLDC****      | 0.35 | 451                                   | 350                                 | 0.3                         | 550                         | -                | 0.5              |

\*NFRNWC: Non-Fibre Reinforced Normal Weight Concrete

\*\*NFRLDC: Non-Fibre Reinforced Low Density Concrete

\*\*\*SFRLDC: Steel Fibre reinforced Low Density Concrete

\*\*\*\*PFRLDC: Plastic Fibre reinforced Low Density Concrete

### 4 SPECIMEN PREPARATION

All concrete specimens were cast and cured in accordance with ASTM C192. A total of 5 specimens including three 100.6 x 203.2 mm cylinders and two 150 x 150 x 530 mm prisms were prepared for each mixture. The mixing procedure consisted of firstly mixing all aggregates (fine and coarse) for 30 seconds. This was followed by the addition of cement, EPS beads and fibres, which were then mixed for 30 seconds, 1 minute and 2 minutes, respectively. Water was then added and left to mix for another 3 minutes. The superplasticizer was finally added to achieve the desired workability. Concrete specimens were then cast after which the specimens were covered in wet burlap and plastic for 24 hours. The specimens were then demoulded and placed in a fog room (100% relative humidity) at room temperature (22±2°C) until they were tested.

### 5 TEST SETUP AND PROCEDURE

#### 5.1 Compression test

The compressive strength test was performed on 100.6 x 203.2 mm cylinders in accordance with ASTM C39 at a loading rate of 35 psi/sec (0.24 MPa/sec). Compressive strength was measured at an age of 28 days.

#### 5.2 Flexural test

The flexural strength (average of two specimens) was measured on the form finished side of 150 x 150 x 530 mm prisms under four-point loading configuration in accordance with ASTM C1609/C1609M-12. Two LVDTs were mounted on a jig at mid-span, one on each side in order to measure the displacement. The jig was clamped to the prism directly above the supports. The tests were carried out at a constant loading rate of 0.1mm/min in accordance with table 1 in ASTM C1609/C1609M-12 before and after a net deflection of L/900 (where L = 457.2 mm) had been reached. A photograph of the test setup is presented in Figure 1.

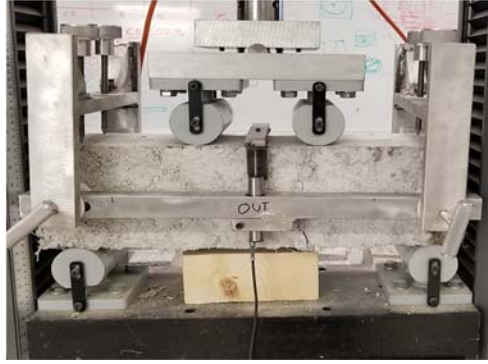


Figure 1: Test Setup for Flexural test.

### 5.3 Digital image correlation

DIC is a non-contact optical full-field deformation measurement system. A commercial, 3D acquisition and analysis software was used for this research (Correlated Solutions Vic-3D and Vic Snap). It was used to measure the displacement and strain on the specimens. The setup consists of two cameras with a resolution of 5 megapixels positioned 300 mm apart on a tripod and 1000 mm away from the specimen in such a way that the specimen fills the field of view of both cameras. An external light source was used to illuminate the field of view. Necessary adjustments to focus, aperture and exposure time were made to ensure higher image quality. Prior to testing, the specimen surface in view of the camera was painted white and speckled with random black dots. The system was then calibrated as specified by vic-3d testing guide. Images were captured at one frame per second. Applied force data was also recorded with a data acquisition system coupled to the DIC software during testing. Analysis and post-processing of data was done with image analysis software with a subset size of 35 pixels. Figure 2 and 3 presents the speckled specimens prior to testing and the DIC test setup, respectively.

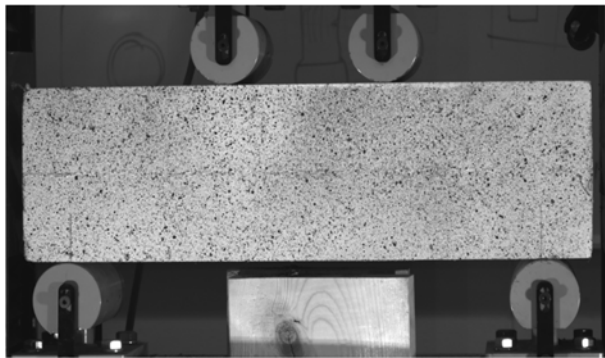


Figure 2: Speckle pattern on specimen



Figure 3: DIC setup

## 6 RESULTS AND DISCUSSIONS.

### 6.1 Fresh concrete properties (Slump)

The workability of each mixture was determined by measuring the slump in accordance with CSA A23.2-5C. The results are presented in Table 3 and show that the workability decreased with addition of fibres and improved with higher content of superplasticizer.

### 6.2 Density

The density of each mixture was determined in accordance with CSA A23.2-11C and are presented in Table 3. The addition of fibres is shown to have negligible effect on the hardened concrete density, which is not surprising considering the volume replacement was less than 1%. The density of the low density mixes show a 20% decrease from the normal weight concrete mix.

### 6.3 Compressive strength

The compressive strength following 28 days of age is also presented in Table 3. The results show that the addition of steel fibres slightly increases the compressive strength. However, the addition of plastic fibres showed a 3% decrease in 28-day compressive strength. This decrease can be attributed to the tendency of plastic fibres to agglomerate in the mix, which can introduce air voids in the specimen. The addition of fibres also showed an improvement in post peak ductility capacity of the concrete specimens.

### 6.4 Flexural strength

The flexural strength was determined and calculated in accordance with ASTM C1609 and are presented in Table 3. It was observed that the addition of fibres increased the flexural strength. However, the use of steel fibres gave a significantly higher flexural strength when compared with the plastic fibre and non-fibre mixes as expected. Typical flexural load-deflection curves for the different mixes used in this study are presented in Figure 4-6, which compares the load-deflection plots of the DIC and that from LVDT. Increase in flexural strengths beyond a displacement of 1.5mm is attributed to strain hardening due to the effects of fibres. Both curves correspond with each other and proves the validity and reliability of the use of DIC to measure displacement and strain values. The DIC was used for measurement on one of the prisms while the LVDT was used for the other. Both methods were not combined as the jig holding the LVDT was in the view of the camera.

Table 3: Concrete Properties

| Concrete | Density (kg/m <sup>3</sup> ) | Compressive Strength (MPa) | M.O.R (MPa) | Slump (mm) |
|----------|------------------------------|----------------------------|-------------|------------|
| NFRNWC   | 2408                         | 65                         | 3.79        | 45         |
| NFRLDC   | 1930                         | 31                         | 2.71        | 65         |
| SFRLDC   | 1933                         | 33                         | 3.87        | 70         |
| PFRLDC   | 1929                         | 30                         | 3.14        | 25         |

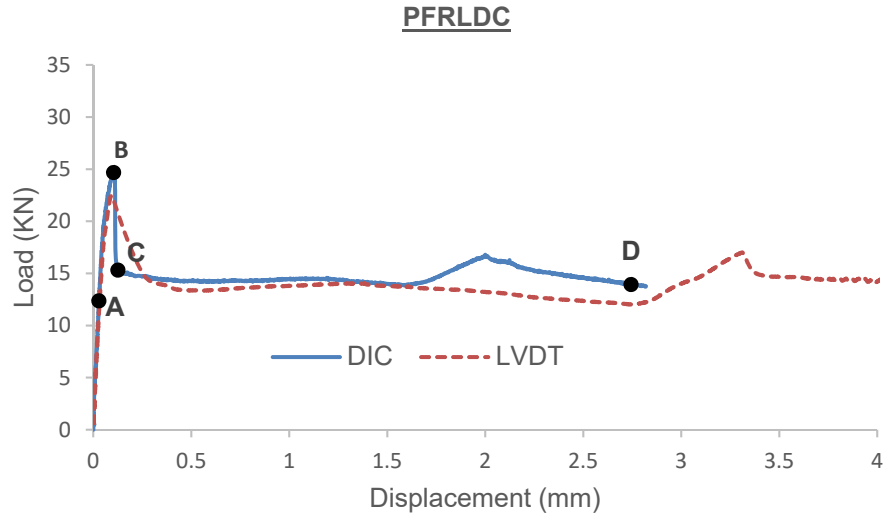


Figure 4: Load-Displacement curve for plastic fibre reinforced low-density concrete

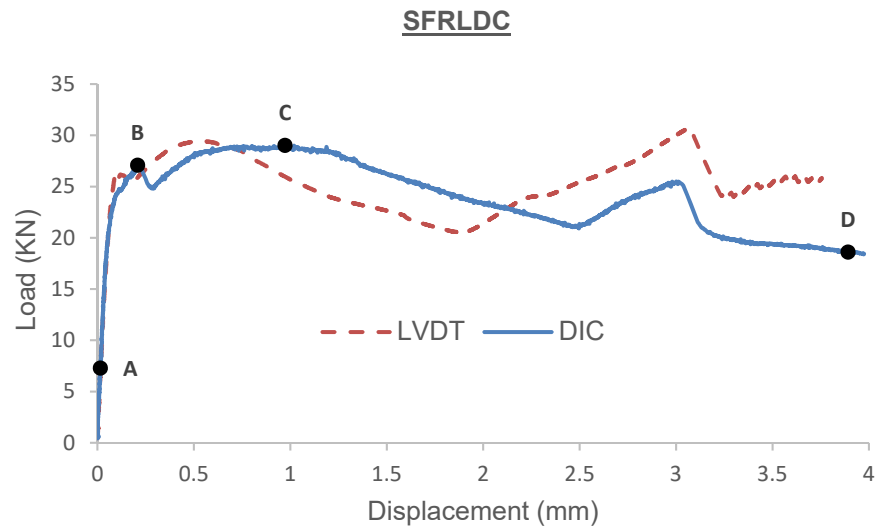


Figure 5: Load-Displacement curve for steel fibre reinforced low density concrete

## NFRLDC

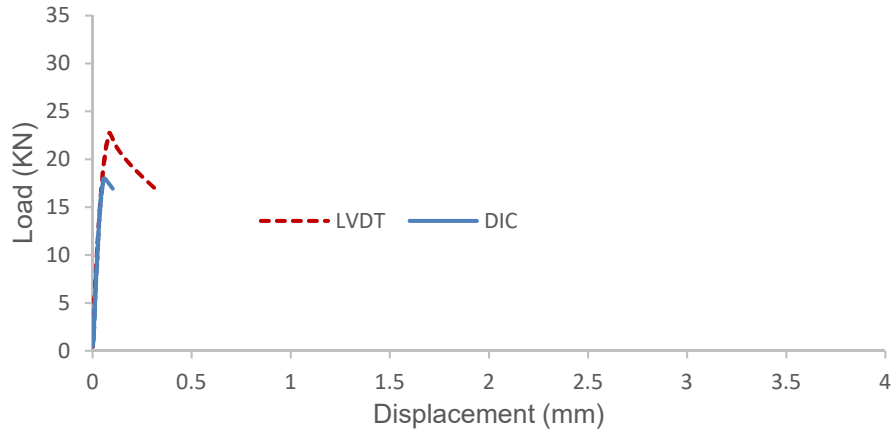


Figure 6: Load-Displacement curve for non-fibre low density concrete

### 6.5 Crack detection

Cracking in concrete is most times a sign of failure. This can be seen when a concrete specimen is subjected to constant loading. Due to these loads it is capable of reaching its capacity, which inevitably leads to cracking and in certain cases failure. In bending tests, as cracks propagate, there is a decrease in load and increase in crack width. It is assumed that the point of divergence from linearity of load-deflection curves is the point of first crack (Bensaid et al., 2014). Though this assumption holds value, it is still difficult to identify these cracks especially in cases where multiple cracks exist. In bending tests, these cracks develop in the tensile region of the specimen and propagate upwards towards the loading surface. With the aid of DIC, the cracks were immediately detected and their propagation was monitored until failure as presented in Figure 7. The figure shows the longitudinal (strains due to flexure) strain fields overlaid on the prisms at various times as the flexural test proceeded to specimen failure. Regions on the beam indicated by red show high strain concentrations and existence of cracks, whereas purple indicates low strain values (compression). From the image analysis, it was observed that SFRLWC (Figure 7 left) had more than one crack. The primary (first) crack corresponds with the deviation from linearity on the load deflection curve and was bridged by fibres. A secondary crack developed which led to the ultimate failure of the beam. Figure 7 shows the detection and propagation of cracks on the steel and plastic fibre concrete mixes studied. Figure 7A represents the strain distribution at the linear-elastic region. Figure 7B represents the first crack and initiation of cracks. Figure 7C shows the propagation of crack and Figure 7D shows the fracture of the specimens. These can also be seen in the load-deflection plots in figures 4 and 5.

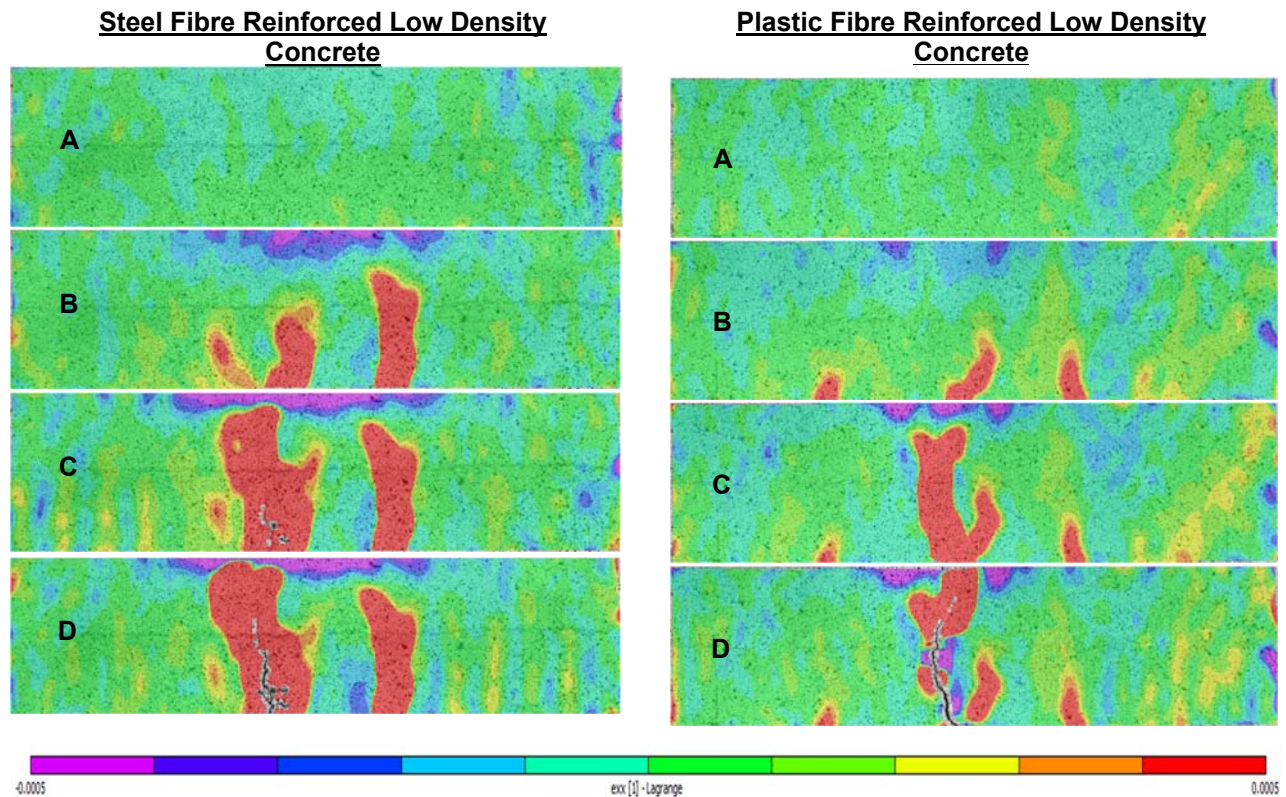


Figure 7: Contour diagram showing longitudinal strain distribution.

## 6.6 Neutral axis movement

The neutral axis is defined as an axis in the cross-section of a beam where stresses and strains are zero. If the beam cross-section is symmetric and the material is homogeneous and isotropic, the neutral axis would be at the centre. However, when concrete specimens are loaded, cracks develop causing the material to be anisotropic and the neutral axis shifts. By using image analysis, the shift of neutral axis of the concrete beams was observed. It was observed that the plastic fibre mix showed a high jump in the neutral axis position when cracks developed when the sectional strain was measured at the crack location. This can also be seen in the load-deflection curve (Figure 4) where there was a rapid drop in load after first crack. However, the movement of the neutral axis in the SFRLDC mix was gradual as a result of the fibres arresting the crack and the high flexural strength of the matrix. When cracks developed, the neutral axis moved up and was measured to be 49.4mm from the compression face of the beam as shown in Figure 9. This movement was gradual until failure and was measured to be 33.2 mm at fracture. The neutral axis position in the non-fibre mix is not presented in this work. From Figures 8 and 9, it can be seen that the strain distribution of the compression side remained largely linear. The strain distribution in the tension side is not representative of the real material strains due to the formation of cracks in the tension zone. From the movement of the neutral axes, strain diagrams were plotted considering only compression strain values with line of best fit extending into the tension region and are presented in Figure 10 and 11.

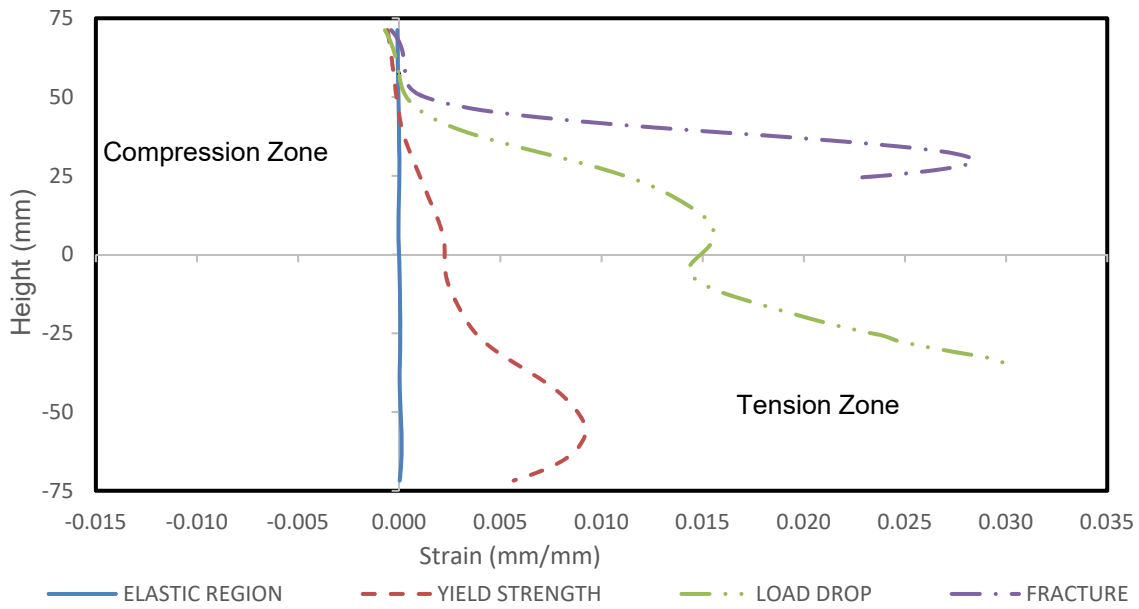


Figure 8: Neutral axis movement of PFRLDC shown from DIC

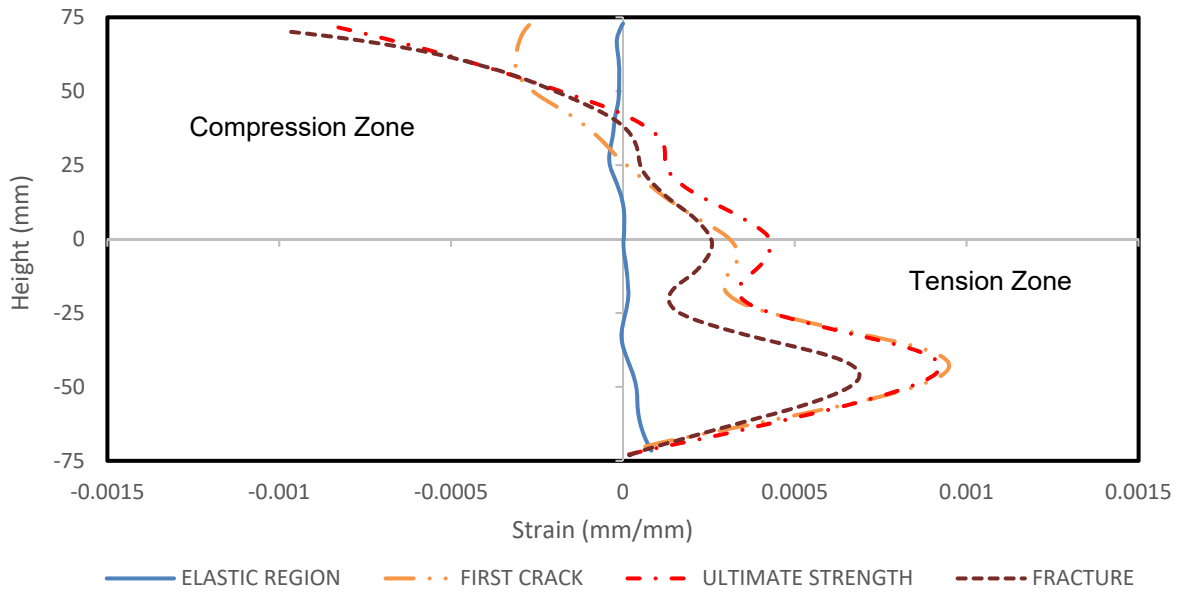


Figure 9: Neutral axis movement of SFRLDC shown from DIC

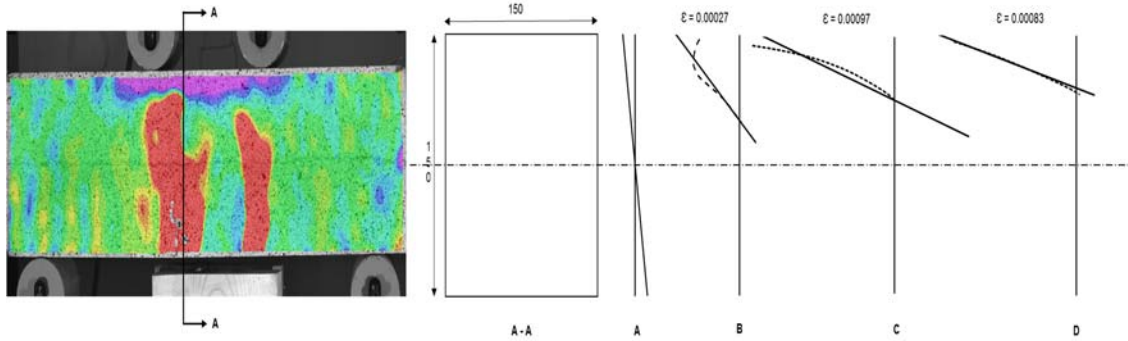


Figure 10: Neutral axis movement of SFRLDC plotted from DIC

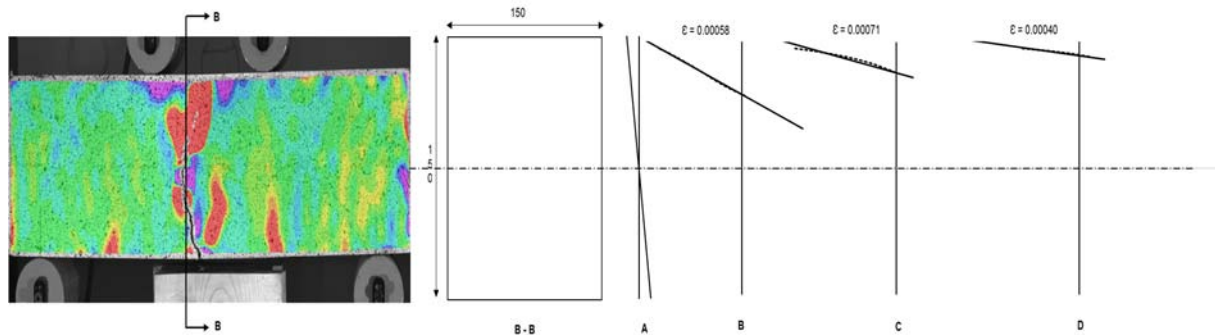


Figure 11: Neutral axis movement of PFRLDC plotted from DIC

Table 4a: Neutral axis position for SFRLDC

| Point | Position          | Distance* (mm) |
|-------|-------------------|----------------|
| A     | Elastic region    | 75             |
| B     | Yield Strength    | 49.40          |
| C     | Ultimate Strength | 36.85          |
| D     | Fracture          | 33.20          |

Table 4b: Neutral axis position for PFRLDC

| Point | Position       | Distance* (mm) |
|-------|----------------|----------------|
| A     | Elastic region | 75             |
| B     | Yield Strength | 31.08          |
| C     | Load Drop      | 18.14          |
| D     | Fracture       | 8.08           |

\* Distance measured from the compression face of the specimen.

Based on the results presented within this paper, the following conclusions can be drawn:

- The effectiveness of steel fibres in arresting cracks is more pronounced than plastic fibres. This can be seen from the neutral axis plots where the steel fibre mix showed a gradual shift in neutral axis position compared to plastic fibre, which showed a more rapid movement.
- Steel fibre of low aspect ratio and volume fraction as low as 0.5% produces tensile hardening properties when used in low density concrete.
- The use of steel fibres slightly improved the compressive strength and greatly improved the flexural strength and ductility of the matrix.
- Digital image analysis is effective and a more accurate way of measuring deformation and fracture.

## References

ACI 211.2. 2004. Standard practice for selecting proportions for structural lightweight concrete. ACI International. Moraga Dr, Los Angeles, United States.

- ACI 544.1R. 2010. State of the art report on fibre reinforced concrete. ACI International. Moraga Dr, Los Angeles, United States.
- ASTM C1609/C1609M. 2012. Standard test method for flexural performance of fiber-reinforced concrete (using beam with third-point loading), *ASTM International*. West Conshohocken, PA, United States.
- Bensaid B., Mostefa H., Mohamed C. and Sofiane A. 2014. Failure mechanism of fibre reinforced concrete under splitting test using digital image correlation. *Materials and Structures*, no. 48: 2713–2726
- Correlated Solutions. 2016. Vic-3D v7.2.6 Testing guide.
- Correlated Solutions. 2016. Vic-3D v7.2.6 Reference Manual.
- Grédiac. 2004. The use of full-field measurement methods in composite material characterization: Interest and limitations. *Applied Science and Manufacturing* 35(7-8):751-761.
- McCormick, N. and Lord J. 2010. Digital Image Correlation. *Materials Today* 13, no. 12: 52–54.
- Rizzuti, L. and Bencardino, F. 2014. Effects of Fibre Volume Fraction on the Compressive and Flexural Experimental Behaviour of SFRC. *Contemporary Engineering Sciences* 7, no. 8: 379-390.
- Robins. P, Austin, S. and Jones, P. 2002. Pull-out Behaviour of Hooked Steel Fibres. *Materials and Structures* 35, no. 7: 434–42.
- Song, P. S and Hwang, S. 2004. Mechanical Properties of High-Strength Steel Fiber-Reinforced Concrete. *Construction and Building Materials* 18, no. 9: 669–73.
- Wu, Y., Jie, L., and Keru W. 2004. Mechanical Properties of Hybrid Fiber-Reinforced Concrete at Low Fiber Volume Fraction. *Cement and Concrete Research* 33, no. 1: 27–30.